

PERSPECTIVES IN FUNDAMENTAL AND APPLIED RHEOLOGY

EDITED BY:

F.J. RUBIO - HERNÁNDEZ

A.I. GÓMEZ - MERINO

C. DEL PINO

L. PARRAS

L. CAMPO - DEAÑO

F.J. GALINDO - ROSALES

J.F. VELÁZQUEZ - NAVARRO

“NOTICE: this is the author’s version of a work that was accepted for publication in the Book **Perspectives in Fundamental and Applied Rheology**. Changes resulting from the publishing process, such as peer review, editing, corrections, structural formatting, and other quality control mechanisms may not be reflected in this document. A definitive version is available in the Book **Perspectives in Fundamental and Applied Rheology**, Rubio-Hernández, F. J., et al. (Eds), 2013.

Separation and deformation of red blood cells in PDMS microchannels

Raquel O. Rodrigues¹, Vera Faustino^{1,2}, Diana Pinho^{1,2}, Elmano Pinto^{1,2}, Diana Cidre¹, Tomoko Yaginuma¹, Bruna Taboada^{1,2}, David Bento^{1,2}, Rui Lima^{1,2}

¹ ESTiG, Polytechnic Institute of Bragança, C. Sta. Apolónia, 5301-857 Bragança, Portugal.

² CEFT, Faculty of Engineering, University of Porto, R. Dr. Roberto Frias, 4200-465 Porto, Portugal.

Introduction

Over the years, several experimental techniques were performed in *in vitro* environments, in an attempt to understand the flow behaviour of blood in microcirculation. Several of these studies were performed in glass capillaries, and have produced significant results with respect to rheological properties of blood [1, 2]. Another way to perform *in vitro* blood studies is to use microchannels fabricated by soft- lithography [3, 4] and xurography [5]. With these techniques several studies have focused in the formation of the cell-free layer (CFL) that is caused by the tendency of red blood cells (RBCs) to migrate toward the centre of the microchannel, in that the physical reason is known as the Fahraeus Lindqvist. The presence of this CFL at the regions adjacent to the wall is affected by the geometry of the microchannel [4] and the physiological conditions of the working fluid, such as the hematocrit (Hct) [6], and the RBC deformability [7]. The

formation of CFL can be used for separation of diseased cells from healthy blood cells [8]. The aim of this paper is to show briefly the importance of the microfluidic devices to study several physiological phenomena that happens *in vivo* environments with special focus on the CFL behaviour and RBC deformability.

Materials and Methods

Working fluids

Generally several working fluids were examined: dextran 40 (Dx-40) containing 1%, 5%, 9% and 12% of RBCs. The hematocrits (Hcts) correspond to the feed reservoir Hct and it was measured by using a hematocrit centrifuge. Detailed description of the samples preparation can be found elsewhere [4, 5, 9-11].

Microchannels fabrication

The microchannels tested were fabricated by means of two different microfabrication techniques, i. e., the soft-lithography [3, 4] and soft-xurography [5]. All the microchannels tested with dimensions less than 200 μm were fabricated by standard soft-lithography techniques from a SU-8 photoresist mold [4, 9-11]. Recently we have developed a low cost microfabrication technique to study blood flow phenomena at a microscale level. This process uses vinyl mold masters fabricated by a cutting plotter. By using this technique we do not need a clean room facility and as a result it is possible to reduce significantly the production cost. Figure 1 shows the vinyl mold master and the correspondent PDMS microchannel fabricated by a soft-xurography. Detailed description of this fabrication process can be found elsewhere [5].

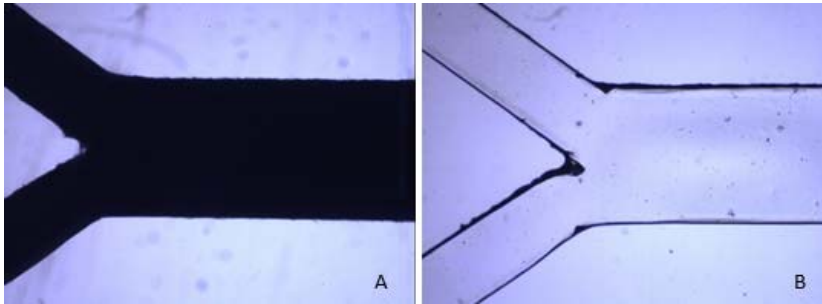


Figure 1. Images obtained using an inverted microscope with a 4x objective lens: A - The vinyl mold master fabricated by a cutting plotter; B – PDMS microchannel of the confluence.

Experimental set-up.

The high-speed video microscopy system used in our experiments consists of an inverted microscope combined with a high-speed camera (see Figure 2). The PDMS microchannel was placed on the stage of the microscope where the flow rate of the working fluid was kept constant by means of a syringe pump.

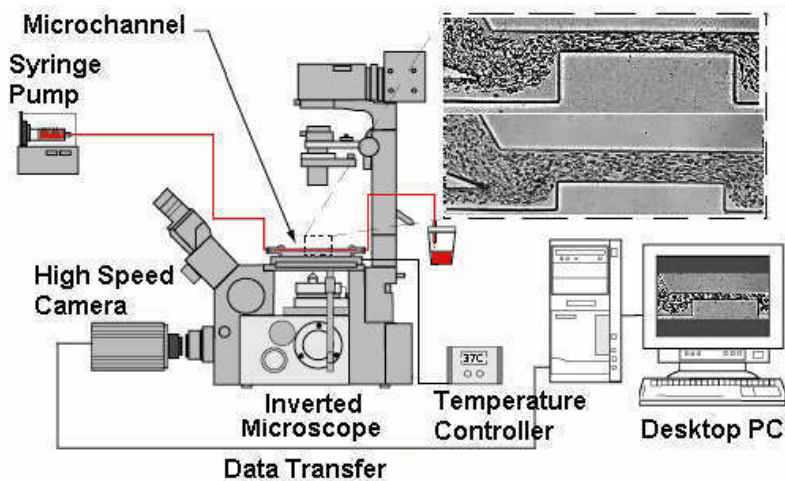


Figure 2. High-speed video microscopy system.

Image analysis

Overall, the recorded images were transferred to the computer and then evaluated in Image J (NIH). To measure the CFL thickness the captured videos were converted to a sequence of static images (stack). Then, for each pixel, the maximum intensity of all the images in the stack was selected using the “Z project” function in ImageJ, which results in a region of RBCs core brighter than the background. To obtain quantitative measurements the grey scale images were converted to binary images with thresholding.

The RBC deformation measurements in hyperbolic microchannels were possible by using the following image analysis procedure. First, the captured videos were converted to a sequence of static images. Then, in order to reduce the noise in the images, a background image was created and subtracted from all original images. This process resulted in images having only the RBCs visible. To enhance its quality, image filtering was applied using ImageJ (NIH). Finally, the grey scale images were converted to binary images adjusting the threshold level. Detailed description of the image analysis procedure can be found elsewhere [10].

Results and Discussion

CFL and RBC separation

By using a microchannel with a confluence fabricated by a soft lithography technique we have obtained a very interesting blood flow phenomenon that happens at microscale level. Figure 3 shows flow visualizations around the confluence on the both trace particles in pure water and human RBCs containing about 14% Hct [4].

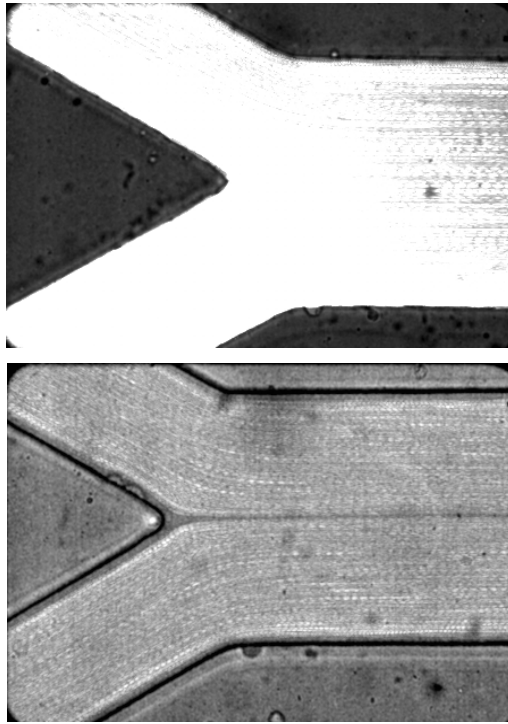


Figure 3. Image of trace particles in pure water (up) and in vitro blood (down) obtained after “Zproject” (maximum intensity function). This microchannel was fabricated by a soft lithography technique.

From Figure 3 we can clearly observe a CFL in middle of the microchannel after the apex of the confluence. In contrast this flow phenomenon is not observed with pure water. Recently, this phenomenon was also observed in microchannels fabricated by a soft xurography technique [5]. Detailed studies about this phenomenon are currently under way and will be published in due time. Figure 4 shows an image with the flow of RBCs through a 75% constriction for a constant flow rate of 1 $\mu\text{L}/\text{min}$. Measurements on the CFL thickness were also performed in a 25% constriction.

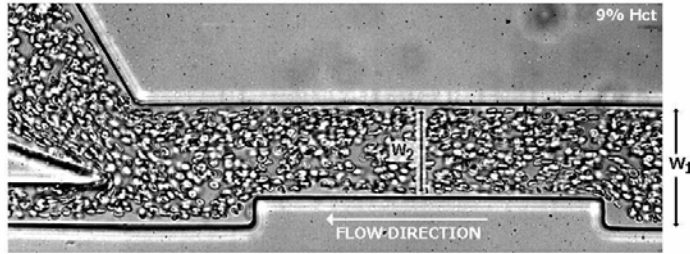


Figure 4. Flow visualization of in vitro blood in a microchannel with the following dimensions: $W_1 = 100 \mu\text{m}$ and $W_2 = 75 \mu\text{m}$.

By using a combination of image analysis techniques we are able to automatically measure the CFL thickness before and after the artificial contractions. Figure 5 shows clearly that in both cases the constriction enhances CFL thickness. Furthermore, it is also clear that the enhancement is more pronounced for the channel with a contraction ratio (W_2/W_1) equal to 0.25 than 0.75 [11]. This separation strategy will be crucial to obtain a low Hct and consequently perform cell deformability measurements.

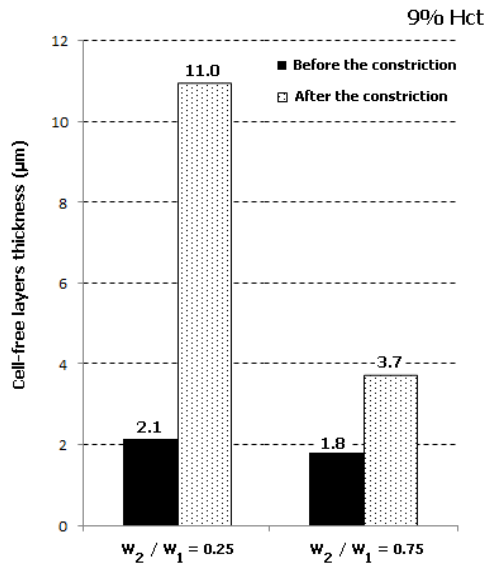


Figure 5. CFL thickness before and after artificial constrictions with different contraction ratios (Hct = 9%) [11].

RBC deformation

To analyze the deformability of RBCs, the cells were measured in two pre-defined regions, (A) and (B) as shown in Figure 6. Region (A) is located upstream of the hyperbolic contraction and region (B) comprises a narrow part of the contraction region. Both regions are located axially along the centerline of the channel.

The flowing cells selected for measurement are measured twice in region (A) and (B). The RBC deformation was defined by the deformation index (DI) as $(L_{Major} - L_{Minor}) / (L_{Major} + L_{Minor})$, where L_{Major} and L_{Minor} refer to the major (primary) and minor (secondary) axis lengths of the ellipse best fitted to the cell. These values were obtained by using ImageJ (NIH).

Figure 6 shows an original image of the PDMS hyperbolic microchannel and the view of flowing RBCs at different flow rates (9.45 $\mu\text{l}/\text{min}$ and 66.15 $\mu\text{l}/\text{min}$) and in two pre-defined regions, (A) and (B). In Figure 7 the average deformation index calculated are shown for each case.

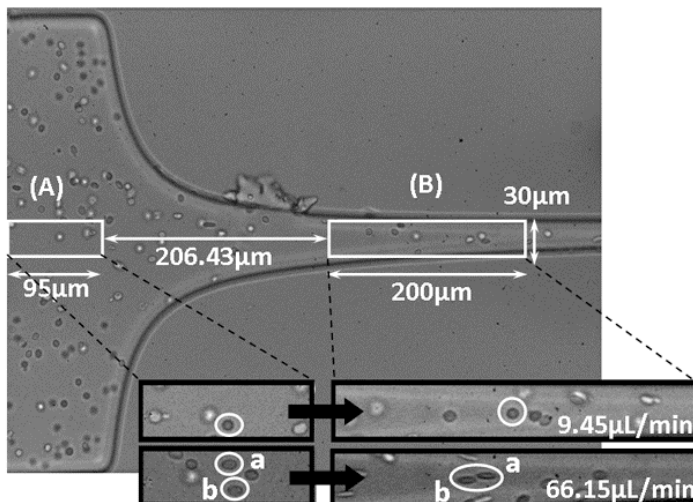


Figure 6. RBC deformation at different flow rates in region A and B [9].

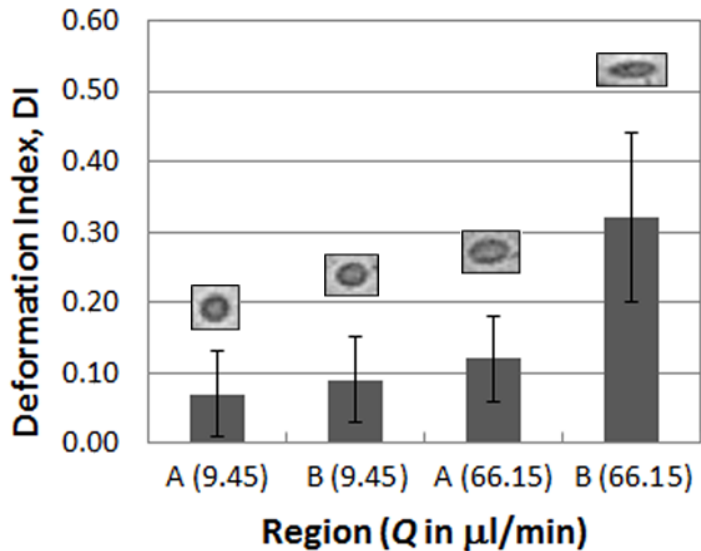


Figure 7. Comparison of deformation index at different flow rates in different regions.

As can be seen in Figure 7, for both flow rates, DI is higher in the hyperbolic contraction region (B) where the RBCs are submitted to a strong extensional flow. In the contraction region (B), DI increases substantially with the flow rate as a consequence of the higher strain rate to which the RBCs are submitted. These results evidence the highly deformable nature of RBCs under strong extensional flows and the present hyperbolic-shape microchannel is suitable for RBC deformability examination.

Acknowledgment

The authors acknowledge the financial support provided by: PTDC/SAU-BEB/108728/2008, PTDC/SAU-BEB/105650/2008, PTDC/EME-MFE/099109/2008 and PTDC/SAU-ENB/116929/2010 from FCT (Science and Technology Foundation), COMPETE, QREN and European Union (FEDER).

References

1. Lima, R., Ishikawa, T., Imai Y., and T., Yamaguchi T. (2012). In Single and two-Phase Flows on Chemical and Biomedical Engineering (Dias, R., Martins, A.A., Lima, R. and Mata, T.M. eds.), 513–547, Bentham Science Publishers: Netherlands.
2. Garcia, V., Dias, R. and Lima, R., (2012). In Applied Biological Engineering – Principles and Practice (Ganesh, R. Naik ed.), Vol. 17, 394-416, InTech.
3. Lima, R., Wada, S., Tanaka, S., Takeda, M., Ishikawa, T., Tsubota, K., Imai, Y. and Yamaguchi, T. (2008). *Biomedical Microdevices*. 10, 153-167.
4. Leble, V., Lima, R., Dias, R.P., Fernandes, C.S., Ishikawa, T., Imai, Y., and Yamaguchi T. (2011). *Biomicrofluidics*. 5, 044120.
5. Pinto, E., Pinho D., Bento, D., Correia, T., Garcia, V., Dias, R., Miranda, J.M. and Lima, R. (2013). *5°CNB*, 301-306.
6. Kim, S., Ong, P.K., Yalcin, O., Intaglietta, M., and Johnson, P.C. (2009). *Biorheology*. 46, 181-189.
7. Fujiwara, H., Ishikawa, T., Lima, R., Matsuki, N., Imai, Y., Kaji, H., Nishizawa, M. and Yamaguchi, T. (2009). *J. Biomech*. 42, 838-843.
8. Hou, H.W., Han, J. and Lima, C.T. (2010). *Lab.Chip*. 10, 2605-2613.
9. Yaginuma, T., Oliveira, M.S.N., Lima, R., Ishikawa, T., Yamaguchi, T. (2011). *Microtech Conference and Expo Boston, MA, USA, 2*, 505.
10. Yaginuma, T., Oliveira, M.S.N., Lima, R., Dias, R., Ishikawa, T., Imai, Y., Yamaguchi, T. (2012). *ECCOMAS Thematic Conference on Computational Vision and Medical Image Processing* 209-211.
11. Lima, R., Oliveira, M.S.N., Yaginuma, T., Ishikawa, T., Imai, Y., Yamaguchi, T. (2011) *Japan-Portugal Nano-Biomedical Engineering Symposium*. 1, 49-50.